Microwave imaging device prototype for brain stroke 3D monitoring

Microwave Imaging Device Prototype for Brain Stroke 3D Monitoring

J. A. Tobon Vasquez*, D. O. Rodriguez-Duarte*, C. Origlia*, G. Turvani*, R. Scapaticci†, M. R. Casu*, L. Crocco†, F. Vipiana*

*Dept. Electronics and Telecommunications, Politecnico di Torino, Torino, Italy,
{jorge.tobon, david.rodriguez, cristina.origlia, giovanna.turvani, mario.casu francesca.vipiana}@polito.it

†Institute for the Electromagnetic Sensing of the Environment, National Research Council of Italy, Naples, Italy,
{scapaticci.r, crocco.l}@irea.cnr.it

***Abstract*—This paper summarizes the development and the experimental testing of a scanning device, in the microwave range, to monitor brain stroke. The device comprehends 4 main sections: a sensors helmet, a switching matrix, a data acquisition part, and a control/processing core. The sensors in the helmet are 22 custom-made flexible antennas working around 1 GHz, placed conformally to the upper head part. A first validation of the system consists in the detection of a target in the head region. Experimental testing is performed on a single-cavity head phantom, while the target is a balloon mimicking the stroke. The shape of the balloon and phantom are extracted from medical images, and tissues properties are emulated with liquids that resemble their dielectric properties. A differential measurement approach senses the field on the antennas in two different situations, and from their difference computes a 3-D image through a singular value decomposition of the discretized scattering operator obtained from an accurate numerical model. The results verify the capabilities of the system on detecting and monitoring stroke evolution.**

***Index Terms*—Microwave imaging, biomedical imaging, microwave antenna array, flexible antenna, hemorrhagic stroke, numerical simulation, propagation.**

I. Introduction

Brain stroke causes 5 million deaths and permanent damages in surviving patients each year [1]. A rapid and accurate diagnosis, and monitored therapy could ameliorate that scenario.

Currently, physicians follow the first stages of stroke evolution through imaging and patient behavioural parameters. The imaging techniques used are mainly Magnetic Resonance Imaging (MRI) or X-ray-based Computerized Tomography (CT). These well-assessed techniques could bring some drawbacks for continous monitoring in the stroke first stages. MRI machine size, cost, and no wide-availability together with CT ionizing radiation, and the time required for both to prepare patients or process data, push research community to look for alternatives or complementary technologies. Microwave imaging (MWI) techniques could fill the gap left by MRI and CT in bedside monitoring, ambulance diagnosis, and continous information on the evolution of the stroke.

This work was supported by the Italian Ministry of University and Research under the PRIN project "MiBraScan", and by the European Union's Horizon 2020 research and innovation program under the EMERALD project, Marie Skłodowska-Curie grant agreement No. 764479.

Some solutions using Microwave technology have been already developed in recent years [2]–[4], following two different approaches: classification with no images ([3]) and quantitative imaging ([2]). The classification requires a large dataset of previously measured data, while the imaging leads to higher computational times and more complex systems.

In [5] the authors presented a first iteration of the designed device, with both numerical [6] and experimental validation [7]. The low-complexity aim is pursued here reducing the size of the sensors helmet, and using flexible antennas that permit a better coupling with patients head.

We are interested in a localized region of the brain where and when the stroke is changing, it permits to keep the complexity of the problem and the processing time low. This localized nature of the scenario allows the Born approximation [8], [9] to linearize the differential problem.

II. System Description

The scheme of the implemented prototype (in fig.1) comprehends four main sections: antennas on the head, switching matrix (routing of the signal), the signal generation/acquisition system (VNA), and the control and data processing core (where the imaging algorithm is implemented).

A. Antennas Helmet

The antenna here presented is an evolution on the brick-shaped antenna in [10], aiming to optimize the performance in the proximity of the human head, while reducing the size of the helmet and making it actually wearable. The antenna is made from two layers of flexible and custom material, together with a low-complexity monopole element. One of the flexible layers acts as substrate of the printed antenna (between printed monopole and ground plane), while the other serves as matching medium, reducing the mismatch between antenna and head. The radiator part is printed on flexible commercial polymide film, and the antenna is back-fed. The tuning of the mentioned custom materials reaches an appropppriate trade-off between high permittivity and low losses. Table I describes

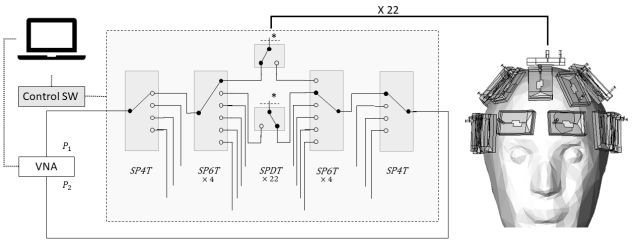

Fig. 1. Scheme of implemented device prototype

TABLE I
MATERIALS COMPOSITION AND PERMITTIVITY

	Graphite [%]	Rubber [%]	–	ϵ_r (1 GHz)	σ [S/m]
Matching	75	25		13	0.18
Substrate	65	35		18	0.3
	Triton X-100[%]	Water [%]	Salt [g/l]	ϵ_r (1 GHz)	σ [S/m]
ICH	14	86	9.4	68	1.5
Brain	38	62	5.2	45	0.7

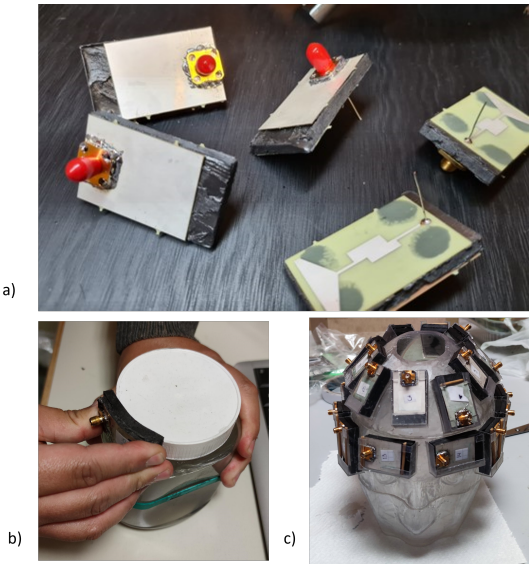

Fig. 2. Flexible antennas. a) Some of the built antennas, matching layer remove to show radiation part; b) bending test; c) antennas around head phantom

the used materials, and their dielectric properties. The complete antenna module has enough flexibility to adapt to head curvature. This module is optimized to work in a -10 dB band from 0.85 to 1.25 GHz, in agreement with the requirements for this application [9]. The number of antennas (22) and position in the upper part of the head are both selected following the design procedure in [9]. Fig. 2 shows antenna details and final array around head.

B. Generation,Acquisition and Routing of Signal

In this prototype we are using a compact 2-port P9375A Keysight Streamline USB VNA. It generates and receives all the signals. The power is set to -5 dBm and the intermediate frequency (IF) filter to 10 Hz to reduce the measurement noise. Two coaxial cables connect VNA to ports of the switching matrix. This switiching system is made of high-isolation electromechanical coaxial switches, linking each of the 22 antennas to the VNA ports when required. Semi-rigid coaxials improve the isolation between each layer of switching. In a scan each antenna will work as transmitter and receiver, obtaining all the possible combinations of the 22 antennas, and generating a complete scattering matrix. Low cost and high availability of off-the-shelf devices in the microwave range could permit a final device implementation that substitutes VNA or other system stages with ad-hoc solutions. The speed of the switching matrix could be improved going towards a solid-state solution.

C. Imaging Algorithm

A personal computer is the control and processing core. Although control permits the functioning of the system, here we focus in the section related to MWI.

The monitoring of the strokes over time leads to a differential approach ([9], [11]). We define ΔS as the difference between scattering matrices collected at two different stroke situations. With the stroke evolving, ΔS changes, containing the information that will be our input data. The output of our algorithm is a 3D image of the variation of the dielectric contrast inside ($\Delta\chi$) the brain under analysis. This differential contrast is the ratio between the permittivity variation between two instants, and the permittivity of the background at the reference instant ($\Delta\epsilon/\epsilon_b$).

As stated before, the localized nature of the contrast variation $\Delta\chi$ allows us to use the Born approximation [12]. The link between ΔS and $\Delta\chi$ becomes:

$$\Delta S\left(\boldsymbol{r}_p, \boldsymbol{r}_q\right) = \mathcal{S}\left(\Delta\chi\right) \tag{1}$$

where $\mathcal{S}$ is linear compact integral operator, with kernel $-j\omega\epsilon_b/A\,\boldsymbol{E}_{\mathrm{b}}\left(\boldsymbol{r}_m, \boldsymbol{r}_p\right)\cdot\boldsymbol{E}_{\mathrm{b}}\left(\boldsymbol{r}_m, \boldsymbol{r}_q\right)$, with $\boldsymbol{r}_m$ the points in the imaging domain D, $\boldsymbol{r}_p$ and $\boldsymbol{r}_q$ the positions of the antennas, A is a "normalizing" constant related to the power applied at the antenna ports. $\omega = 2\pi f$ is the angular frequency, and j the imaginary unit, and the symbol "$\cdot$" denotes the dot product between vectors $\boldsymbol{E}_{\mathrm{b}}$ is the field radiated by antenna of the array to the scenario in abscense of target. These background fields $\boldsymbol{E}_{\mathrm{b}}$ are obtained through simulation using a 3D vectorial finite element method (FEM) and a numerical model of the head-helmet system. To invert (1), we use the well-assessed truncated singular value decomposition (TSVD) scheme [12], obtaining the unknown differential contrast

$$\Delta\chi = \sum_{n=1}^{L_t} \frac{1}{\sigma_n}\left\langle \Delta S, \left[u_n\right]\right\rangle \left[v_n\right], \tag{2}$$

where $\left\langle\left[u\right], \left[\sigma\right], \left[v\right]\right\rangle$ are the results of a singular value decomposition applied on the discretized operator $\mathcal{S}$. The truncation index L_t works as a regularization parameter, avoiding ill-

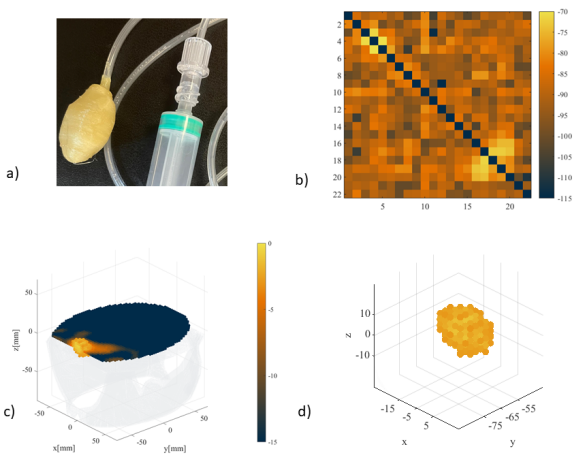

Fig. 3. Experimental test case: (a) Target (stroke of 10 ml) to be detected and filling system; (b) Differential scattering matrix; (c) 3D view of detected target and one transverse plane, amplitude normalized of the reconstructed dielectric contrast; (d) normalized reconstructed dielectric contrast values above -3 dB.

possedness of the inverse operator while keeping a good accuracy.

III. Experimental Results

In the previous section we described the implemented prototype. In this section we will present some results performed in a realistic phantom. As we are in a development stage of the device, we use a *phantom* (object that mimics a body part's characteristics) to test its performance. A phantom gives us total control on the region of interest, and high flexibility in the test cases definition. We fill a human head shaped 3D-printed single-cavity container (fig. 2) with a liquid mimicking the brain tissues' average ("Brain" in Table I). The used target resembles in size and characteristics a hemorrhagic stroke (fig. 3 and "ICH" in Table I), and was obtained from actual medical images. Phantom design and liquids recipes are available at [13]

Measurements are performed in two steps, each related to a stroke situation. In this work we present a presence/absence test, it means one of the "stroke situations" is the phantom with no target, while the other includes the target. The difference between the scattering matrices of the two situations is the input for the TSVD algorithm. Results in Fig. 3, show that the system is capable of accurately localize the pathology while offering a good estimation of the size and shape.

A total scan of the head is performed in around 4 minutes for each of the two differential measurements, but a non-prototypal solution could improve this time. The linearized operator is calculated offline, and the TSVD data processing takes less than 1 s.

IV. Conclusion and Perspectives

This work describes a system for brain stroke monitoring and its experimental testing. A novel flexible and compact antenna is proposed here, reducing the helmet size and improving the contact between sensor and area under test. The complete system gives a good estimation of the location and shape of the target, with a resolution around half centimeter.

Some preliminary tests with "stroke situations" that monitor the growing of the target are being performed, and results will be presented in the conference.

In the next research activities, we will go towards a multi-frequency approach of the imaging, and we will implement a more complex and realistic phantom that considers the multi-tissue nature of the human head.

Acknowledgment

We thank Prof. N. Joachimowicz, Sorbonne University, and Prof. P. Plaisance and Eng. V, Lemarteleur, Ilumens Health Simulation Center, for providing the medical images and the fruitful discussions on the medical aspects and on the modeling manufacturing of the phantoms.

References

[1] E. J. Benjamin, P. Muntner, and M. S. Bittencourt, "Heart disease and stroke statistics-2019 update: a report from the american heart association," *Circulation*, vol. 139, no. 10, pp. e56–e528, 2019.

[2] M. Hopfer, R. Planas, A. Hamidipour, T. Henriksson, and S. Semenov, "Electromagnetic tomography for detection, differentiation, and monitoring of brain stroke: A virtual data and human head phantom study." *IEEE Antennas Propag. Mag.*, vol. 59, no. 5, pp. 86–97, Oct. 2017.

[3] A. Fhager, S. Candefjord, M. Elam, and M. Persson, "Microwave diagnostics ahead: Saving time and the lives of trauma and stroke patients," *IEEE Microwave Mag.*, vol. 19, no. 3, pp. 78–90, May 2018.

[4] A. S. M. Alqadami, K. S. Bialkowski, A. T. Mobashsher, and A. M. Abbosh, "Wearable electromagnetic head imaging system using flexible wideband antenna array based on polymer technology for brain stroke diagnosis," *IEEE Trans. Biomed. Circuits Syst.*, vol. 13, no. 1, pp. 124–134, Feb. 2019.

[5] J. A. Tobon Vasquez, R. Scapaticci, G. Turvani, G. Bellizzi, D. O. Rodriguez-Duarte, N. Joachimowicz, B. Duchêne, E. Tedeschi, M. R. Casu, L. Crocco, and F. Vipiana, "A prototype microwave system for 3D brain stroke imaging," *SENSORS*, vol. 20, no. 9, 2020.

[6] D. O. Rodriguez-Duarte, J. A. T. Vasquez, R. Scapaticci, L. Crocco, and F. Vipiana, "Assessing a microwave imaging system for brain stroke monitoring via high fidelity numerical modelling," *IEEE Journal of Electromagnetics, RF and Microwaves in Medicine and Biology*, vol. 5, no. 3, pp. 238–245, 2021.

[7] D. O. Rodriguez-Duarte, J. A. Tobon Vasquez, R. Scapaticci, G. Turvani, M. Cavagnaro, M. R. Casu, L. Crocco, and F. Vipiana, "Experimental validation of a microwave system for brain stroke 3-d imaging," *Diagnostics*, vol. 11, no. 7, 2021. [Online]. Available: https://www.mdpi.com/2075-4418/11/7/1232

[8] R. Scapaticci, O. Bucci, I. Catapano, and L. Crocco, "Differential microwave imaging for brain stroke follow up," *Int. J. Antennas Propag.*, vol. 2014, no. Article ID 312528, p. 11 pages, 2014.

[9] R. Scapaticci, J. A. Tobon Vasquez, G. Bellizzi, F. Vipiana, and L. Crocco, "Design and numerical characterization of a low-complexity microwave device for brain stroke monitoring," *IEEE Trans. Antennas Propag.*, vol. 66, pp. 7328–7338, Dec. 2018.

[10] D. O. Rodriguez-Duarte, J. A. Tobon Vasquez, R. Scapaticci, L. Crocco, and F. Vipiana, "Brick shaped antenna module for microwave brain imaging systems," *IEEE Antennas and Wireless Propagation Letters*, 2020.

[11] J. A. Tobon Vasquez, R. Scapaticci, G. Turvani, G. Bellizzi, N. Joachimowicz, B. Duchêne, E. Tedeschi, M. R. Casu, L. Crocco, and F. Vipiana, "Design and experimental assessment of a 2D microwave imaging system for brain stroke monitoring," *Int. J. Antennas Propag.*, no. Article ID 8065036, p. 12 pages, 2019.

[12] M. Bertero and P. Boccacci, *Introduction to Inverse Problems in Imaging*. Inst. Phys., Bristol, U.K., 1998.

[13] N. Joachimowicz, B. Duchêne, C. Conessa, and O. Meyer, "Anthropomorphic breast and head phantoms for microwave imaging," *Diagnostics*, vol. 85, no. 8, pp. 1–12, Dec. 2018.